Translocation of "Rod-Coil" Polymers: Probing the Structure of Single Molecules within Nanopores

Hendrick W. de Haan and Gary W. Slater

Physics Department, University of Ottawa, Ottawa, Ontario, Canada K1N 6N5

(Received 25 June 2012; published 23 January 2013)

Using simulation and analytical techniques, we demonstrate that it is possible to extract structural information about biological molecules by monitoring the dynamics as they translocate through nanopores. From Langevin dynamics simulations of polymers exhibiting discrete changes in flexibility (rod-coil polymers), distinct plateaus are observed in the progression towards complete translocation. Characterizing these dynamics via an incremental mean first passage approach, the large steps are shown to correspond to local barriers preventing the passage of the coils while the rods translocate relatively easily. Analytical replication of the results provides insight into the corrugated nature of the free energy landscape as well as the dependence of the effective barrier heights on the length of the coil sections. Narrowing the width of the pore or decreasing the charge on either the rod or the coil segments are both shown to enhance the resolution of structural details. The special case of a single rod confined within a nanopore is also studied. Here, sufficiently long flexible sections attached to either end are demonstrated to act as entropic anchors which can effectively trap the rod within the pore for an extended period of time. Both sets of results suggest new experimental approaches for the control and study of biological molecules within nanopores.

DOI: 10.1103/PhysRevLett.110.048101 PACS numbers: 87.15.ap, 82.35.Lr, 82.35.Pq

Given both the biological relevance and technological applications, the translocation of a polymer through a nanopore has received considerable attention in recent years [1,2]. Experimentally, the focus has been on the passage of DNA through either biological or synthetic nanopores as a means of sequencing [3]. Correspondingly, the bulk of the theoretical and simulation research has focused on polymers of a uniform stiffness

However, there does exist a class of polymers in which there are sudden changes in the local stiffness. As shown in Fig. 1, an example of key interest is strands of partially melted DNA in which the melted portions, consisting of two single strands (ss), are much more flexible than the double-stranded (ds) ones [4]. Another biologically relevant example is given by proteins that primarily consist of alpha-helices where the tertiary structure has been broken but the secondary structure left intact such that the resulting "polymer" is comprised of stiff, alpha helical sections joined by flexible loops comprised of amino acids forming no set secondary structure [5]. There are also numerous examples of block copolymers where stiff sections of type A are joined via flexible sections of type B [6]. Borrowing from the terminology used to describe these complexes, we refer to the generic polymer we study here as a "rod-coil" polymer. Rod-coil type structures are also found in emerging nanotechnology. Examples include polymer analogues composed of gold rods joined together via flexible polymers [7] as well as novel DNA sequencing technology such as a single strand of DNA hybridized at specific locations to yield ss-ds complexes [8] and DNA analogues where rigid sections corresponding to bases are joined by long, flexible sections [9]. Other notable experimental examples include the translocation of DNA-PNA complexes [10] and the translocation of DNA partially coated with the RecA protein in which the RecA regions are significantly stiffer [11].

In this work, we simulate the passage of a generalized rod-coil polymer through a short nanopore. We find that distinct phases in the dynamics directly correspond to changes in the local polymer stiffness indicating that structural information can be extracted by monitoring the translocation process. The discrimination between rod-coil sections is shown to be strengthened for tighter pores or varying charge densities between segments. We also examine the special case of a single rod with coils on either end and show that even short coils present significant entropic barriers impeding its escape from the pore. Such entropic anchors may represent a way to indefinitely confine rigid polymers within a nanopore.

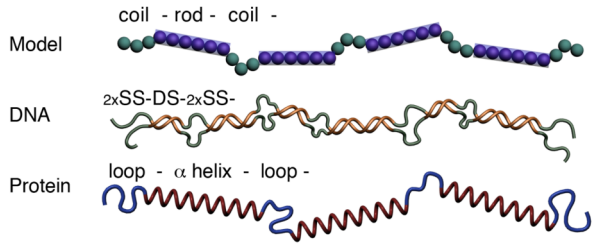

FIG. 1 (color online). Simulation model and biologically relevant examples of rod-coil polymers.

For the simulations, we employ a standard Langevin dynamics (LD) methodology [12]. The Weeks-Chandler-Andersen potential is used for monomer-monomer and monomer-pore excluded volume interactions [13]. The pore is defined to have an effective width that is twice the monomer size σ. A FENE potential is employed to bind monomers along the polymer backbone [14]. For the stiff portions of the polymer, a three-body harmonic interaction with an equilibrium angle of 180° is used. Using a force constant of 100 kT/σ yields a persistence length of 100σ and thus even the longest rod studied, $M_{\mathrm{rod}} = 40$, is very stiff. Our (coil-rod)$_{N_{\mathrm{rod}}}$-*coil* polymers, where N_{rod} is the number of rods, always have coils on their ends. As shown in Fig. 1, this simple model yields a generic rod-coil polymer. While analogous to a variety of real polymers (both biological and synthetic) that exhibit discrete changes in stiffness, there are of course many details missing when comparing to any particular example. Hence, in this study, we investigate the impact of discrete changes in stiffness on the translocation dynamics in a general sense with a generic polymer model; while the underlying concepts are then applicable to any particular experimental case, the details will of course affect the realized effects.

For the initial configuration, we assume a polymer with M monomers has been "captured" to the extent that the initial flexible portion of length M_{coil} has been translocated with the first bead of the first rod just entering the pore. Mimicking the application of an external field E, a driving force $F = qE$, where q is the charge on the monomer, is applied towards the *trans* side to any monomer in the pore. Generally all monomers carry the same charge $q = 1$ such that $F = E$. Considering applications such as α helices connected by short loop sections or DNA that is only partially denatured, the rod sections are set to be longer than the coil sections by an arbitrarily chosen factor of two. While the data is not shown, we have also conducted simulations with a 1:1 ratio between the rod and coil sections. Results consistent with the data and analysis presented below were obtained. As shown in Table I, we construct simulations for different numbers of rods while attempting to keep constant the total number of monomers which must be translocated, $M_{\mathrm{trans}} = M - M_{\mathrm{coil}}$. Note that as any two consecutive monomers can be considered a "rod," the limiting case where a coil is one monomer and a rod is two monomers is identical to a freely jointed chain.

TABLE I. Parameters for the simulations. The last column gives the height for the local entropic barriers in units of kT.

M	M_{trans}	N_{rod}	M_{rod}	M_{coil}	h
80	60	1	40	20	3.86
70	60	2	20	10	3.57
70	63	3	14	7	3.33
64	60	5	8	4	2.77
62	60	10	4	2	1.82
61	60	20	2	1	0

The efficacy of the methodologies outlined below rely on discrete changes in the free energy due to changes in the entropic cost of translocation progressing. The effects are most dramatic when the system is close to being *quasistatic* such that the polymer is always relaxed. This limit corresponds to the friction of the monomers moving through the pore being dominant over friction through the bulk: the polymer moves through the fluid easily, relaxes quickly, and the bottleneck step is getting through the pore. To move the system towards this limit, one can lower the viscosity of the fluid or reduce the pore diameter. To begin, we present results for a low effective fluid viscosity $\tilde{\eta} = 0.1$ [15,16]. Use of this quasistatic limit not only allows for better discrimination between rod and coil segments, but also presents a scenario that is more readily solved by analytic means.

To characterize the dynamics, we employ the incremental mean first passage time (IMFPT) approach that we have developed in recent papers [16,17]. Here, we simply keep track of the first time, labeled $t_0(s)$, that the monomer s is in the pore ($s \in [1, M]$; $s = 1$ being the head of the polymer). The results for $N_{\mathrm{rod}} = 3, 5, 10, 20$ at a driving force of $\tilde{F} = 0.5$ (where $\tilde{F}$ is a dimensionless force defined to be $F\sigma/kT$) are shown in Figs. 2(a)–2(f) in red. The progression of t_0 follows distinct steps. When a rod is in the pore, s increases rapidly and the curve has a shallow slope. However, at the end of each rod, there is a large jump in the time required for translocation to proceed indicating that there is a significant energy barrier at this transition point.

To probe these barriers, an analytic technique is employed. In the quasistatic limit, we take the free energy landscape to be constant in order to calculate the translocation time following the approach of Sung and Park, and Muthukumar [18,19]. Recently we extended this formulation to calculate the incremental mean first passage time [17] for s,

$$t_0(s) \sim \int_0^s ds' e^{\beta U(s')} \int_0^{s'} ds'' e^{-\beta U(s'')}, \qquad (1)$$

where $U(s)$ is the free energy. The results shown in Figs. 2(a)–2(f) suggest a corrugated free energy landscape with barriers at the location of the coils. To model this, we simply increase the free energy by an amount h whenever a coil is in the pore. The overall entropic barrier is also included. As in the early work of Sung and Park, and Muthukumar, the free energy is given by:

$$U(s) = -kT \ln\left(\frac{1}{(M-s)^{1-\gamma}} \frac{1}{s^{1-\gamma}}\right) + U_0(M), \qquad (2)$$

where $\gamma = 0.69$ is the surface exponent for self-avoiding polymers [20] and $U_0(M)$ is a constant that will be neglected hereafter. Using this form for the current study,

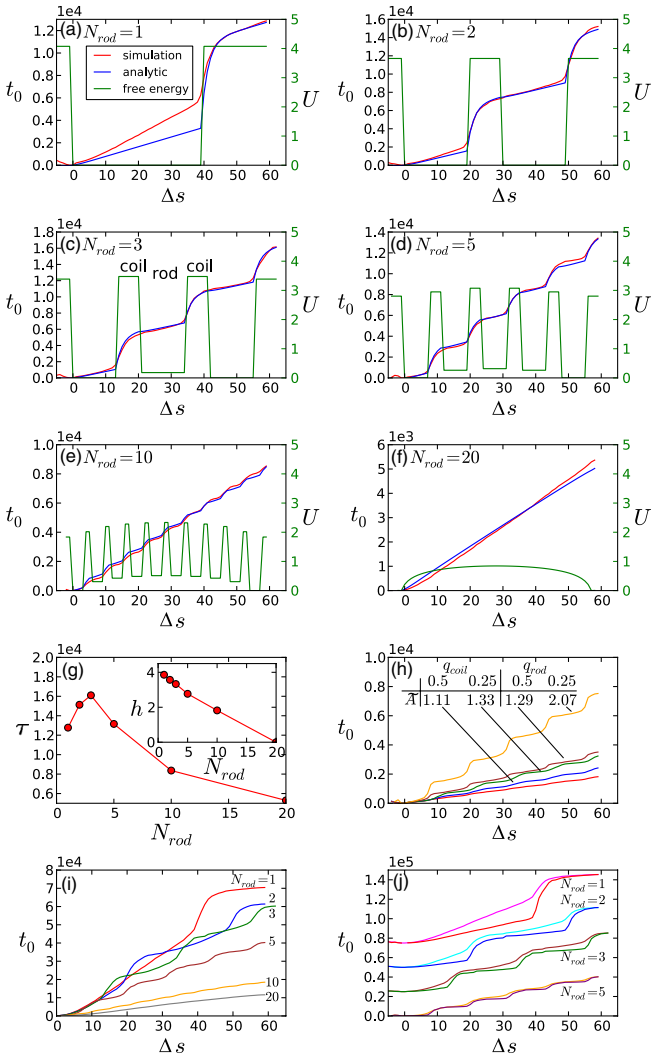

FIG. 2 (color online). IMFPT data for rod-coil polymers. (a)–(f) display the $\tilde{\eta} = 0.1$, $\tilde{F} = 0.5$ simulation (red) and analytic (blue) results along with the free energy profile in units of kT (green, axis on the right) for $N_{\mathrm{rod}} = 1$, 2, 3, 5, 10, 20, respectively. In (g) the net translocation time τ is plotted against N_{rod} for $\tilde{F} = 0.5$. The inset shows the scaling of the barrier height h with the number of rods N_{rod} in units of kT. (h) displays the results for differing q_{coil} and q_{rod} as well as the case when all monomers carry charge $q = 1$ (red) at $\tilde{F} = 2$. (i) displays the simulation results for all N_{rod} cases at $\tilde{\eta} = 1$ at $\tilde{F} = 0.5$. The $N_{\mathrm{rod}} = 1$, 2, 3, 5 cases are shown in (j) for both a wide pore (upper line in each pair) and tight pore (lower line). The $N_{\mathrm{rod}} = 1$, 2, 3 cases have been shifted vertically by 7.5×10^4, 5×10^4, and 2.5×10^4 respectively and the wide pore results have been normalized to match the end points of the tight pore results.

each rod and coil section is counted as one monomer in the calculation of the global entropic barrier. For the rods, this choice is justified by considering that they have no internal degrees of freedom. For the coils, the additional entropic cost is counted through the local entropic barriers h. $U(s)$ is then constructed by combining the global and local entropic barriers [as shown in Figs. 2(a)–2(f)]. A term U_F arising from the driving force is also included in the potential calculation. With an external field E applied across the pore, the net energy gain starting from $s = 1$ and being at s is $U_F = -\sum_{i=1}^{s-1} q_i E\sigma$ where q_i is the charge on monomer i.

To compare the analytical formulation with the simulation results, it is necessary to match the time scales. As discussed, the $N_{\mathrm{rod}} = 20$ case is equivalent to a freely jointed chain and thus there is no entropic mismatch between rod and coil sections such that $h = 0$. As shown in Fig. 2(f), using a prefactor of 34 for Eq. (1) is then found to give good agreement. With the prefactor fixed, the height of the local entropic barrier h is the only free parameter in the model. Values for h were determined by minimizing the difference between the analytic and simulation results. The good agreement shown in Figs. 2(a)–2(e) confirms the presence of barriers introduced by the sudden entropic cost of confining the coils within the pore. Further, the excellent agreement that is obtained for the cases $N_{\mathrm{rod}} = 2$, 3, 5, 10 validates the analytic approach. Most obviously, the analytic and simulation results match in terms of discrete jumps in the dynamics yielding the staircase pattern for t_0. Moreover, the agreement for the rate of translocation during the rod phase and the curvature during the coil phase is remarkable considering the simple step potential used. For further verification, the potentials were also explicitly measured yielding good agreement as expected (see Supplemental Material [21]).

As indicated by the last column in Table I, the resulting barrier height h can be several times kT. Plotting the barrier height against the number of rods [inset to Fig. 2(g)], there is a systematic decrease in the barrier heights for polymers consisting of a greater number of rod sections. Hence, given a particular polymer size M, the height of the local barriers decreases with an increasing number of repeating units.

In applying a constant force F to any monomer in the pore, we have thus far assumed that each monomer carries the same charge q such that $F = qE$. However, depending on the particular polymer under study, it is conceivable that the linear charge density could also change between rod and coil sections. We therefore conducted simulations where the charge on rod monomers, q_{rod}, and coil monomers, q_{coil}, differ. Keeping E fixed, changing the charge scales the magnitude of the force applied to monomers in the pore. First, we set $q_{\mathrm{rod}} = 1$ while q_{coil} is reduced to 0.5 and then 0.25. This was then reversed with $q_{\mathrm{coil}} = 1$ while q_{rod} is reduced. The results are shown in Fig. 2(h) for the high external field case $E = 2$. While the case when all monomers carry the same charge is nearly featureless (red), lowering the charge on either the rod or coil sections increases the translocation time and brings out structural features. As we are lowering the net charge on the polymer, an increase in the translocation time is not unexpected.

However, if this were the only factor, one would expect $\tau \sim 1/F \sim 1/Q$ where Q is the total charge. To test this, we define a normalized prefactor $\tilde{A} = \frac{\tau Q}{\tau_0 Q_0}$ where τ_0 and Q_0 are the net translocation time and net charge when all monomers carry $q = 1$. This data is included as a table in Fig. 2(h). When the charge on the coil is reduced, the proportional increase in τ is not very large: 11% and 33% for $q_{\text{coil}} = 0.5q$ and $0.25q$. However, $\tilde{A}$ not being equal to one demonstrates that the interplay between the driving force and the entropic effects is nonlinear. The result is more dramatic for the cases where the charge on the rod is decreased. For $q_{\text{rod}} = 0.25q$, $\tilde{A}$ is over two. The physical picture here is that although the local entropic barrier corresponding to translocating a coil is independent of q_{rod}, reducing q_{rod} reduces the frequency of "attempts" to translocate the coil and thus the translocation time greatly increases.

Figure 2(i) displays the IMFPT results for $F = 0.5$ and $\tilde{\eta} = 1$. While features corresponding to the molecular structure are still evident, it is clear that moving away from the pore friction dominated limit reduces the resolution. Note also that, contrary to the $\tilde{\eta} = 0.1$ results [Fig. 2(g)], τ now decreases monotonically with increasing N_{rod}. To sharpen the features, the same simulations were performed with a tighter pore such that the effective diameter is 1.2 (down from 2). The results for the $N_{\text{rod}} = 2, 3, 5$ cases are shown in Fig. 2(j) along with the corresponding results for the wider pore. Narrowing the pore increases the resolution of the structural features as expected: the wide pore results appear as a fuzzy envelope of the sharp, narrow pore results. It is important to note that while these results indicate that a narrower pore will enhance the effect, in an experimental scenario, the increased interaction between the polymer and the pore can introduce additional effects (such as "sticking") which can complicate the net result.

Additional simulations were performed at $N_{\text{rod}} = 1$ with M_{rod} held at 30 and M_{coil} varying from 1 to 30. We refer to these flexible-rigid-flexible structures as "Q-Tips" (see schematic in Fig. 3). To bring these results closer to experimental conditions, the viscosity has raised to $\tilde{\eta} = 1$. The results for $\tilde{F} = 0$ are shown in Fig. 3 (note that as $\tilde{F} = 0$, the polymer is now initiated half-way through the pore). Three distinct regimes are apparent. From the initial position up to the end of the rod at $\Delta s = \pm 15$ translocation proceeds at a moderate rate that increases slowly with M_{coil}. On entry of an end coil to the pore, there is a large jump in the time. The size of this jump increases sharply with M_{coil}. Following this large initial barrier, there is a progressive increase in the rate of translocation as the polymer moves toward exiting on either side. Marking $M_{\text{coil}}/2$ on Fig. 3 provides an approximate delineation between these regimes.

These results indicate that having coils attached to a rod inside a nanopore yields a metastable state confining the rods to be in the pore. For a polymer of uniform flexibility, the half-way configuration represents the highest free energy state as the polymer is at the top of the entropic barrier. In contrast, for a rigid rod with entropic anchors, there is a local energy minimum around the half-way configuration: the rod can diffuse back and forth easily, but there are barriers when trying to move the rod out and a coil into the pore.

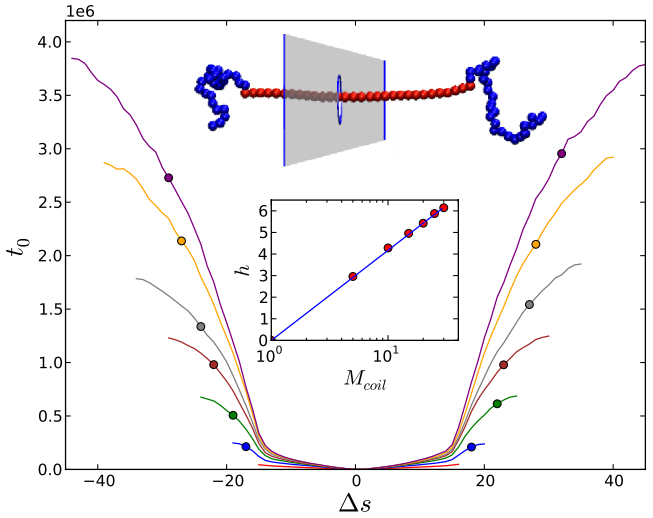

FIG. 3 (color online). IMFPT results for a single rod within a pore for increasing coils lengths: $M_{\text{coil}} = 1$ (red), 5 (blue), 10 (green), 15 (brown), 20 (grey), 25 (orange), 30 (purple) in the absence of a driving force. The locations where either coil is half-way through the pore are marked by circles. The inset shows the estimated barrier height in units of kT for different coil lengths.

To estimate the barrier height, we define an escape time by the total translocation time minus the time required to reach the end of the rod portion: $\tau_e = \tau - \tau_{\text{rod}}$. For the zero field case, τ_e will be expected to follow a Kramer's escape process such that $\tau_e = Ce^{h/kT}$ where C is a prefactor. From this, $h/kT = \ln(\tau_e/C)$. The prefactor C can be set by taking the $M_{\text{coil}} = 1$ case to correspond to a negligible barrier such that $h \approx 0$ and $C = \tau_e(M_{\text{coil}} = 1)$. Then, $h(M_{\text{coil}}) = \ln[\tau_e/\tau_e(M_{\text{coil}} = 1)]$ and these values are plotted in the inset to Fig. 3. In the simplest picture, the number of possible states for the polymer, Ω, grows with the length of the coil section leading to $S \sim \ln\Omega \sim \ln M_{\text{coil}}$; the corresponding barrier height would be expected to follow $h \sim \ln M_{\text{coil}}$ in agreement with the data in the inset to Fig. 3.

We have demonstrated that the entropic mismatch between stiff and flexible sections of translocating polymer gives rise to local entropic barriers. Further, monitoring the dynamics of translocation via an IMFPT analysis can provide direct information about these changes in flexibility. The discrimination between rod and coil sections is most dramatic when pore friction is dominant in determining the rate of translocation. Hence, in the lab, the effect will be

strongest for narrow pores, low viscosity conditions, or polymers of smaller molecular weight. Similarly, differing charge densities between rod and coil segments enhances the resolution, particularly when the charge on the rods is lower than that on the coils. Such an approach may have applications such as determining the melting profile of DNA or probing the secondary structure of proteins using nanopore devices. It was also shown that a single rod can be confined within a nanopore for a significantly extended time period if there are flexible coils attached at either end. Given appropriate experimental conditions, a double stranded segment of DNA could thus be trapped within a pore by having sufficiently long, denatured single stranded AT-rich sections at either end. Likewise, an α helix could be trapped by ensuring there are non-helix forming sections of amino acids at either end.

Another possibility suggested by this work is a technique for generating DNA melting profiles by pulling a partially melted strand of DNA through a nanopore via atomic force microscopy or optical tweezers. Our results indicate that significantly more force will be required to translocate the melted portions and, similar to studies examining the structure of RNA [22,23], the resulting force-extension curves will thus give direct structural information We are currently developing more detailed simulations to investigate these possibilities.

The authors thank Vincent Tabard-Cossa for helpful discussions. Simulations were performed using the ESPRESSO package [24] on the SHARCNET computer system [25]) using VMD [26] for visualization.

[1] B. Alberts, D. Bray, J. Lewis, M. Raff, K. Roberts, and J. D. Watson, *Molecular Biology of the Cell* (Garland Publishing, New York, 1989).
[2] M. Muthukumar, *Polymer Translocation* (CRC Press, New York, 2011).
[3] D. Branton*et al.*, Nat. Biotechnol. **26**, 1146 (2008).
[4] E. Stellwagen, Y. Lu, and N. Stellwagen, Biochemistry **42**, 11 745 (2003).
[5] C. Branden and J. Tooze, *Introduction of Protein Structure* (Garland Publishing, New York, 1998).
[6] M. Lee, B. K. Cho, and W. C Zin, Chem. Rev. **101**, 3869 (2001).
[7] Z. Nie, D. Fava, E. Kumacheva, S. Zou, G. C. Walker, and M. Rubinstein, Nat. Mater. **6**, 609 (2007).
[8] www.nabsys.com.
[9] www.stratosgenomics.com.
[10] A. Singer, M. Wanunu, W. Morrison, H. Kuhn, M. Frank-Kamenetskii, and A. Meller, Nano Lett. **10**, 738 (2010).
[11] S. W. Kowalczyk, A. R. Hall, and C. Dekker, Nano Lett. **10**, 324 (2010).
[12] G. W. Slater, C. Holm, M. V. Chubynsky, H. W. de Haan, A. Dubé, K. Grass, O. Hickey, C. Kingsburry, D. Sean, T. N. Shendruk, and L. Zhan, Electrophoresis **30**, 792 (2009).
[13] J. D. Weeks, D. Chandler, and H. C. Andersen, J. Chem. Phys. **54**, 5237 (1971).
[14] G. S. Grest and K. Kremer, Phys. Rev. A **33**, 3628 (1986).
[15] H. W. de Haan and G. W. Slater, J. Chem. Phys. **136**, 154903 (2012).
[16] H. W. de Haan and G. W. Slater, J. Chem. Phys. **136**, 204902 (2012).
[17] H. W. de Haan and G. W. Slater, J. Chem. Phys. **134**, 154905 (2011).
[18] W. Sung and P. J. Park, Phys. Rev. Lett. **77**, 783 (1996).
[19] M. Muthukumar, J. Chem. Phys. **111**, 10 371 (1999).
[20] E. Eisenriegler, K. Kremer, and K. Binder, J. Chem. Phys. **77**, 6296 (1982).
[21] See Supplemental Material at http://link.aps.org/supplemental/10.1103/PhysRevLett.110.048101 for a direct measurement of the free energy landscapes.
[22] U. Gerland, R. Bundschuh, and T. Hwa, Phys. Biol. **1**, 19 (2004).
[23] R. Bundschuh and U. Gerland, Phys. Rev. Lett. **95**, 208104 (2005).
[24] H. J. Limbach, A. Arnold, B. A. Mann, and C. Holm, Comput. Phys. Commun. **174**, 704 (2006).
[25] www.sharcnet.ca.
[26] W. Humphrey, A. Dalke, and K. Schulten, J. Mol. Graphics **14**, 33 (1996).